Article:

Meng, Q, Liu, F, Fisher, J et al. (1 more author) (2013) Effect of simplifications of bone and components inclination on the elastohydrodynamic lubrication modeling of metal-on-metal hip resurfacing prosthesis. Proceedings of the Institution of Mechanical Engineers, Part H: Journal of Engineering in Medicine, 227 (5). 523 - 534. ISSN 0954-4119

https://doi.org/10.1177/0954411912472845

IMechE Part H: Journal of Engineering in Medicine (accepted version)

The Effect of Simplifications of Bone and Components Inclination on the Elastohydrodynamic Lubrication Modelling of Metal-on-Metal Hip Resurfacing Prosthesis

Qingen Meng [a, *], Feng Liu [a], John Fisher [a], Zhongmin Jin [a, b, *]

[a] Institute of Medical and Biological Engineering,
School of Mechanical Engineering,
University of Leeds, UK

[b] School of Mechanical Engineering,
Xi'an Jiaotong University, China

[*] Corresponding author
Email: qingen.meng@gmail.com, Z.Jin@leeds.ac.uk

Abstract

It is important to study the lubrication mechanism of metal-on-metal (MOM) hip resurfacing prosthesis in order to understand its overall tribological performance, thereby minimize the wear particles. Previous elastohydrodynamic lubrication (EHL) studies of MOM hip resurfacing prosthesis neglected the effects of the orientations of the cup and head. Simplified pelvic and femoral bone models were also adopted for the previous studies. These simplifications may lead to unrealistic predictions. For the first time, an EHL model was developed and solved for a full MOM hip resurfacing arthroplasty. The effects of the orientations of components and the realistic bones on the lubrication performance of MOM hip resurfacing prosthesis were investigated by comparing the full model with simplified models. It was found that the orientation of the head played a very important role in the prediction of pressure distributions and film profiles of the MOM hip resurfacing prosthesis. The inclination of the hemispherical cup up to 45° had no appreciable effect on the lubrication performance of the MOM hip resurfacing prosthesis. Moreover, the combined effect of material properties and structures of bones was negligible. Future studies should focus on higher inclination angles, smaller coverage angle and micro-separation related to the occurrences of edge-loading.

Keywords

Hip resurfacing arthroplasty; lubrication analysis; metal on metal; orientations of cup and head; bone

Introduction

Metal-on-metal (MOM) hip resurfacing arthroplasty has become an attractive method of joint reconstruction for young and active patients due to its theoretical biomechanical advantages [1, 2]. Although significantly lower wear rates have been observed for MOM hip resurfacing prostheses, compared with conventional MOM total hip replacements (THRs) [3-5], some clinical and computational results indicated an opposite trend [6-8]. A Medical Device Alert has been issued for the high failure rate of one type of MOM hip resurfacing prosthesis [9]. Moreover, the size of the metallic particles of MOM hip resurfacing prostheses is as small as that of the THRs (in nanometer) [4]. The ions levels of Cobalt (Co) and Chromium (Cr) in blood or urine of patients with MOM resurfacing prostheses are comparable with those of the patients with THR [10-12]. Furthermore, the life expectancy of the majority of the patients receiving MOM hip resurfacing prosthesis is considerably longer than that of the elderly patients who traditionally receive THRs. Therefore, the concerns raised by the long-term exposure to elevated metal ion levels in the body still exist. These concerns include hypersensitivity, tissue toxicity, carcinogenicity, chromosomal aberration, and the risk of passing chromosomal abnormalities to the next generation [13, 14]. More recently, pseudotumours, caused by edge loading and increased metallic wear particles, have been found in a number of clinical studies of MOM hip resurfacing prosthesis [15-18]. Therefore, metallic particles of MOM hip resurfacing prosthesis have to be minimized to avoid potential adverse biological reactions.

Since wear particles are mainly generated by the direct contact between bearing surfaces, they can be reduced by using bearing materials with high wear resistance. Moreover, a synovial fluid type of lubricant generally forms in the joint capsule after hip arthroplasty. Promoting lubricant protection between the bearing surfaces is also an effective approach to reducing wear, because an effective lubricant film is able to separate the bearing surfaces and reduce the proportion of the load carried by asperity contacts. Therefore, it is important to study the lubrication mechanism in hip resurfacing prostheses. Elastohydrodynamic lubrication (EHL), considering the interaction between the deformation of the bearing surfaces and the hydrodynamic pressure between the bearing surfaces, plays an important role in the study of lubrication mechanism of hip prostheses in terms of accurately predicting film thickness and pressure distribution [19]. The current EHL models applicable to hip replacements can be found in a few review papers [19, 20].

Although a large number of lubrication studies have been performed for THRs [20], only few studies [21-23] have been performed to investigate how design parameters, such as the head diameter, diametric clearance, cup wall thickness and detailed structures and fixation of the femoral component, affect the EHL of MOM hip resurfacing prostheses. These studies assumed that the cup was horizontally positioned and the head was vertically positioned. However, both *in-vivo* and *in-vitro* wear studies of MOM hip resurfacing prostheses suggested the importance of the orientation of the acetabular components [24-29]. Moreover, in these studies, the pelvis and femur were simplified using equivalent bone models with appropriate material properties [21-23]. Although a contact mechanics study has been performed to justify the application of the equivalent bone models [22], the effects of realistic bone structures on the lubrication performance of MOM hip resurfacing prostheses remain unknown due to the lack of a full model that considers the realistic geometries and material properties of the pelvis and femur.

Therefore, the aim of this study was twofold. At first, an EHL model for a full MOM hip resurfacing arthroplasty was developed. In this model, the realistic structures and material properties of bones, components and their fixations were all incorporated. Subsequently, the effects of the orientations of components and the structures of realistic bones on the lubrication were investigated by comparing this full model with simplified models.

Models and Methods

Full model

The full MOM hip resurfacing model (model-f) considered in the present study is shown in Figure 1. The diameter, radial clearance and cup thickness of this surface hip prosthesis were 50 mm, 75 μm and 3.94 mm, respectively [23]. The minimum and maximum thicknesses of the head were 2.5 and 9 mm, respectively. The radius and length of the pin of the head were approximately 3.5 mm and 60 mm, respectively. Both the acetabular and femoral components were made of CoCr alloy with the elastic modulus and Poisson's ratio of 220 GPa and 0.3, respectively. The acetabular component was positioned into the acetabulum with an inclination angle of 45° (β in Figure 2). With a stem to provide the alignment, the femoral component was fixed in the femur using acrylic cement, also with an inclination angle of 45°. No anteversion was considered in the present study. The effect of anteversion will be considered in future studies. The solid models of the hemi-pelvis and the proximal femur were created from CT data [30]. A uniform thickness of 1.5 mm was adopted for the cortical bone of the pelvis [31]. The thickness of the cortical bone of the femur was variable with a maximum value of approximately 4.5 mm. The elastic modulus and Poisson's ratio of the cortical bone of both the pelvis and femur were 17 GPa and 0.3 [32]. The elastic moduli of the cancellous bone of the pelvis and femur were assumed to be 0.5 and 1.5 GPa, respectively. The Poisson's ratio of the cancellous bone of both the pelvis and femur was 0.3 [31, 33]. The elastic modulus, Poisson's ratio and thickness of the acrylic cement mantle were 2.5 GPa, 0.25 and 1.0 mm, respectively [31, 33]. These material parameters are summarized in Table

1. The interfaces between the components and the bone, the femoral component and the cement, and the cement and the bone were assumed to be perfectly bonded to simulate a fully in-grown bone situation or the perfect cement interlocking.

The lubricant in artificial hip joints is periprosthetic synovial fluid. Previous studies showed protein in synovial fluid may play an important role in the film formation of MOM hip implants through two mechanisms, a boundary layer of adsorbed protein molecules augmented by a high-viscosity fluid film generated by hydrodynamic effects [34-36]. However, due to the lack of a full rheological model of the lubricant[37], the effect of protein was not considered in this study. Since the viscosity of the synovial fluid does not change with pressure up to 100 MPa [38] and the pressure levels in artificial hip joints are unlikely to exceed 100 MPa, the synovial fluid can be considered as isoviscous. Moreover, although the synovial fluid behaves as a powerful non-Newtonian fluid under relatively low shear rates, under higher shear rates (~ 10^5/s) likely to be experienced in the hip joint, it can be considered as a Newtonian fluid [39]. Therefore, the synovial fluid was considered as isoviscous and Newtonian. A higher viscosity of 0.01 Pa·s was adopted in the present study to facilitate the numerical process, as compared with a more realistic value of 0.002 Pa·s for the synovial fluid and 0.0009 Pa·s for the bovine serum with a concentration of 25% used in the simulator testing [39].

A ball-in-socket configuration shown in Figure 2 was employed to represent the articulation between the femoral and the acetabular bearing surfaces for the EHL analysis. The walking condition was represented by the three-dimensional (3D) loads and motions [40, 41] applied to the head. Both the loading and velocity were assumed to be steady-state in the present study to reduce computational time.

The governing equations for the lubrication model included the Reynolds equation, the film thickness equation and the load balance equations. The steady-state Reynolds equation governing the hydrodynamic action between two bearing surfaces of hip prostheses took the following form in spherical coordinates [41]:

$$\begin{aligned} &\sin\theta \frac{\partial}{\partial\theta}\left(h^3 \sin\theta \frac{\partial p}{\partial\theta}\right) + \frac{\partial}{\partial\phi}\left(h^3 \frac{\partial p}{\partial\phi}\right) \\ &= 6\eta R_{\mathrm{c}}^2 \sin\theta \begin{bmatrix} -\omega_x\left(\sin\phi\sin\theta\dfrac{\partial h}{\partial\theta} + \cos\phi\cos\theta\dfrac{\partial h}{\partial\phi}\right) \\ +\omega_y\left(\cos\phi\sin\theta\dfrac{\partial h}{\partial\theta} - \sin\phi\cos\theta\dfrac{\partial h}{\partial\phi}\right) \\ +\omega_z\sin\theta\dfrac{\partial h}{\partial\phi} \end{bmatrix} \end{aligned} \tag{1}$$

where p is the hydrodynamic pressure in the bearing; h is the film thickness; η is the viscosity of the periprosthetic synovial fluid; R_{c} is the radius of the cup; ω_x, ω_y and ω_z are the angular velocities of the femoral head around the x, y and z axes, respectively; ϕ and θ are the spherical coordinates, as defined in Figure 3.

The boundary conditions for equation (1) were:

$$p = 0 \ \text{ at the edge of the cup} \tag{2}$$

As shown in Figure 3, the edge of the cup was:

$$\begin{cases} \theta_{\mathrm{in}} = 0, \theta_{\mathrm{out}} = \pi \\ \phi_{\mathrm{in}} = \beta, \quad \phi_{\mathrm{out}} = \pi + \beta \end{cases} \tag{3}$$

where β is the inclination angle of the cups of the models, equal to 45º in the present full hip resurfacing model.

The Swift-Steiber (Reynolds) boundary condition was employed for the continuity of flow and the indication of the film rupture at the outlet:

$$\partial p/\partial \phi = \partial p/\partial \theta = 0 \tag{4}$$

The film thickness consisted of the undeformed gap and the elastic deformation of bearing surfaces due to hydrodynamic pressure:

$$h = R_c - R_h - e_x \sin\theta\cos\phi - e_y \sin\theta\sin\phi - e_z \cos\theta + \delta \tag{5}$$

where R_h is the radius of the head; e_x, e_y and e_z are the eccentricities of the femoral head relative to the cup; δ is the local deformation of the bearing surfaces of the cup and head.

In addition, the external load components, w_x, w_y and w_z, were balanced by the integration of the hydrodynamic pressure:

$$f_x = R_h^2 \int_{\phi_{in}}^{\phi_{out}} \int_{\theta_{in}}^{\theta_{out}} p \sin^2\theta \cos\phi \, d\theta \, d\phi = w_x$$

$$f_y = R_h^2 \int_{\phi_{in}}^{\phi_{out}} \int_{\theta_{in}}^{\theta_{out}} p \sin^2\theta \sin\phi \, d\theta \, d\phi = w_y$$

$$f_z = R_h^2 \int_{\phi_{in}}^{\phi_{out}} \int_{\theta_{in}}^{\theta_{out}} p \sin\theta \cos\theta \, d\theta \, d\phi = w_z \tag{6}$$

Numerical method

A flexibility matrix method able to consider the effects of complex structures of lubrication system [23, 42] was used to solve the above EHL model. The details of the method can be found somewhere else [23]. In brief, the Reynolds equation was solved using a Guass-Seidel scheme with local linearization; the elastic deformation was calculated separately from the Reynolds equation, by the product of the flexibility matrix of the lubrication nodes and the nodal force; the two solution modules exchanged data during an iterative process. The flexibility matrix was obtained by inverting the stiffness matrix, which was obtained through finite element (FE) analysis. The nodal force was obtained by transferring the hydrodynamic pressure according to isoparametric element definition.

Two 3D FE models were generated in I-DEAS (Version 11.0, Siemens PLM Software Inc., Plano, USA) to calculate the stiffness matrices of the nodes on the lubricated surfaces of the acetabular and femoral components (Figure 4). One included the acetabular component and the pelvis, and another incorporated the femoral component and the femur as well as their fixation. The meshes of the inner surface of the cup and the outer surface of the head were matched with the lubrication grid shown in Figure 3. A mesh density of 65 × 65 nodes on the contact surface was used for the present study [21, 23] (The differences in the maximum pressure and central film thickness caused by the increase of mesh density to 91 × 91 were less than 1% and 3%, respectively). The stiffness matrices of the nodes on the lubricated surfaces of the cup and the head were obtained by solving the FE models using Abaqus (Version 6.7 – 1, Dassault Systèmes Simulia Corp., Providence, USA). The structural information of these components was coupled into the lubrication analysis by the flexibility matrices.

It should be noted that when the deformation was calculated, the acetabular and femoral components underwent large bending and translational displacements under pressure. Since only the local deformation of the bearing surfaces should be considered in the EHL analyses [43], the mean large displacements were subtracted from the overall displacements of the surfaces, similar to the approach used in the EHL analysis of connecting-rod bearings [44, 45].

Simplified models

In order to examine the effects of the orientations of components of the hip resurfacing replacement and the structure of bones, three simplified models (model-s1, model-s2, and model-s3) using equivalent bone model were also solved. The detailed structure of the simplified models is shown in Figure 5(a). The elastic modulus and Poisson's ratio of the equivalent bone model were 3.0 GPa and 0.3 [22, 23], respectively. The orientations of the components of the simplified models were different. Model-s1 was the widely-used model for the lubrication analysis of hip resurfacing prosthesis [21-23], of which the acetabular component was positioned horizontally and the femoral component was positioned vertically, as shown in Figure 5(b). Both the cup and the head of model-s2 were inclined with an angle of 45° to simulate an anatomical contact (Figure 5(c)). In model-s3 (Figure 5(d)), the cup was inclined with an angle of 45° but the head was assumed to be vertical as that of model-s1.

Two reference models were also introduced to investigate the effect of the structures of bones. Reference model one (model-r1) is the combination of the realistic femoral part of the full model (Figure 4(b)) and the inclined equivalent pelvic part of simplified model two (model-s2, figure 5(c)). Reference model two (model-r2) is the combination of the realistic pelvic part (Figure 4(a)) and the inclined equivalent femoral part of simplified model two.

The same numerical procedure as described in *Numerical method* was used to solve the EHL of these simplified models. Moreover, the static dry contact mechanics of the simplified models (model-s1, model-s2, and model-s3) were also solved to provide corroboration for the EHL models and also to further investigate the effects of the orientations of the components. 3D FE contact mechanics models were created in NX I-DEAS and solved using Abaqus. For each model, the back of the equivalent bone was fully constrained and a vertical load was applied through the center of the head. The friction between the bearing surfaces was not considered because its effect on the contact pressure in a well lubricated MOM hip bearing is negligible. Moreover, it has also been shown that for a MOM hip bearings, a friction coefficient up to 0.2 did not affect the contact pressure prediction [46]. The difference in the maximum contact pressure caused by the increase of mesh density from 64 × 64 elements to 96 × 96 elements on the contact surface was 7%. The mesh density of 96 × 96 elements on the contact surface was employed for all the dry contact models, resulting in a total of approximately 75, 000 8-node linear hexahedral and 6-node linear tetrahedral elements for each dry contact model. With the cup surface being chosen as the slave surface, the element-based surfaces of the cup and head were defined as a contact pair. “Node to surface” was used as the contact discretization for the contact pair. The contact tracking approach was “small sliding”. The option “adjust = 0.0” was used to avoid the initial overclosure of the surfaces. The key word “CLEARANCE” was used to accurately define the initial gap between the bearing surfaces.

Results

Although a wide range of steady-state load and velocity has been considered for the EHL model, the full model was compared with the simplified models under a condition that only considered the vertical load and flexion/extension rotation since in a walking cycle the load is mainly in the vertical direction and the major velocity is in the flexion/extension direction. The model condition was: $w_x = 0.0$ N, $w_y = 3200.0$ N, $w_z = 0.0$ N, $\omega_x = 2.0$ rad/s, $\omega_y = 0.0$ rad/s and $\omega_z = 0.0$ rad/s. In the dry contact mechanics analyses of the simplified models, correspondingly, only a vertical load of 3200.0 N was applied. Figure 6 shows the contour plots of the hydrodynamic pressure of the full hip resurfacing EHL model and the simplified models under the same conditions. The contour plots of the corresponding lubricant film thickness are shown in Figure 7. Figure 8 is the comparison of the pressure distribution and film thickness on the lines of $\phi = 90°$ and $\theta = 90°$ of the full hip resurfacing EHL model and the simplified models. The dry contact pressure distributions of the three simplified models under the vertical load of 3200 N are plotted in Figure 9. Figure 10 shows the comparison of the pressure distribution and film thickness on the lines of $\phi = 90°$ and $\theta = 90°$ of the full hip resurfacing EHL model and the reference models.

Discussion

It is well known that EHL solutions take long computational time and therefore assumptions are usually made to simplify the problem. For example, previous EHL studies of hip resurfacing prostheses used simple supports to represent bones and ignored the effects of the orientations of prosthetic components [21-23]. The present study attempts to examine the validity of these assumptions.

Under typical EHL conditions, the hydrodynamic pressure is generally expected to be similar to the dry contact pressure since the lubrication film is very thin. Therefore, the comparison between hydrodynamic pressure and dry contact pressure is able to verify the solutions of dry contact mechanics and steady-state EHL models. The hydrodynamic pressure obtained from the full model was verified by comparing indirectly with the corresponding dry contact pressure presented in a previous study [33]. Under the same load of 3200 N, the profile of the hydrodynamic pressure shown in Figure 6(a) was similar to that of the dry contact pressure. Moreover, the maximum hydrodynamic pressure predicted from the EHL model was 21.8 MPa, consistent with the maximum dry contact pressure of 22 MPa [33]. The direct comparison between the hydrodynamic pressure and dry contact pressure of the simplified models of the present study is able to provide more supports for the solutions. It is clear that the profiles and the magnitudes of the hydrodynamic pressures of the simplified models shown in Figure 6 closely resembled those of the corresponding dry contact pressures shown in Figure 9.

The widely-used simplified model with a horizontal cup and a vertical head bone (model-s1) did not predict correct pressure distribution and film thickness for MOM hip resurfacing prosthesis, as indicated in Figures 6 to 8. Obvious differences in both profile and magnitude of pressure distribution and film thickness were found between the full model and model-s1.

As shown in Figure 6, the position of the maximum hydrodynamic pressure predicted from the full model was different from model-s1. This is extremely important because it represents the position of the maximum stress experienced by the components. Moreover, the central film thickness of the full model was significantly thicker than that of model-s1 (Figures 7 and 8). The present findings call for questions in majority of previous lubrication studies reported in the literature, largely based on model-s1.

Model-s2 produced similar hydrodynamic pressure distribution and lubricant film thickness profile to the full model (Figures 6 to 8). Since the only difference between model-s1 and model-s2 was the orientations of the cup and head, this reflected a remarkable effect of the anatomical inclination angle of the cup and head, particularly for resurfacing type prostheses which tend to use thin components. The effects of the orientations of the components can be further examined by comparing the EHL and dry contact mechanics solutions of model-s1, model-s2 and model-s3. The inclination angles of the cups of model-s1 and model-s3 were different, while their heads were positioned in a similar way. Therefore, the comparison between them highlighted the effect of the orientation of the cup component. Since the dry contact pressure and hydrodynamic pressure distribution and lubricant film profile of model-s1 and model-s3 were identical (Figures 6 to 9), the inclination of the cup up to 45° had no effect on the lubrication performance of MOM hip resurfacing prosthesis. This is consistent with the conclusion drawn for the MOM spherical THR from a previous study [47]. It is also reasonable to conclude that the inclination angle of the hemispherical cup (up to 45^o) may have negligible effect on the wear of hip resurfacing prostheses as it did not affect the lubrication performance and contact mechanics of the MOM hip prosthesis. It should also be noted that the contact areas of the cases investigated in this study were all within the cup (away from the edge). However, it should be pointed out that *in-vivo* and *in-vitro* studies [24-29] indicated that steeper acetabular components may cause severe wear. Since the effect of the normal inclination of the cup itself can be excluded from the present study, future studies should concentrate on higher inclination angles, smaller coverage angle and micro-separation related to the occurrences of edge-loading.

In a similar manner, the remarkable differences in the hydrodynamic and dry contact pressures and lubricant film of model-s2 and model-s3 were attributed to the effect of the orientation of the head component, since the inclination angle of the cups of model-s2 and model-s3 was similar, while their heads were positioned in a different way. This is because the stiffness of the head is different at different contact positions due to the non-uniform structures of the head and its fixation. Finally, it can be concluded that the difference in the lubrication performance of model-s1 and model-s2 was caused by the the orientation of the head component. Therefore, it is important to incorporate the correct orientation of the head component in the EHL and contact mechanics models of MOM surface hip prostheses.

Moreover, the agreement between the results of model-s2 and the full model implied that the combined effect of the material properties and structures of the bones on the lubrication performance of MOM hip resurfacing prostheses was negligible. This was consistent with the conclusion drawn from previous studies [21, 23]. Therefore, it is possible to replace the realistic bones using equivalent bone models with appropriate material properties in the EHL models of MOM hip resurfacing prostheses. However, there were still differences in the hydrodynamic pressure and film thickness between model-s2 and the full model. These differences indicated that the material parameters for the equivalent bone model adopted in the present study were not accurate enough to represent the realistic bones. Future studies should be conducted to obtain optimal material properties for the equivalent bone model.

The effect of the structures of the realistic femur and pelvis was also investigated by comparing the full model with reference models. Results shown in Figure 10 indicated that the local fluctuations on the film thickness and pressure in the entraining direction of the full model may be a result of the consideration of the realistic structure of the femoral bone, since both the full model and model-r1 produced local fluctuations in the entraining direction while model-r2 did not. Moreover, the approximate agreement between reference models and the full model confirmed again the possibility to replace the realistic bones using equivalent bone models with appropriate material properties in computational models.

The increasing early failure of MOM hip resurfacing implant has caused concerns. Along with the corrosion between the large metal head and the stem [48], edge loading is an important reason of this early failure [17, 49], because it not only increases the local contact pressure, but also is believed to cause loss of lubrication [24, 50]. Edge loading occurs when the contact patch between the acetabular and femoral components extends over the rim of the cup, which may be caused by a steeply inclined cup and other factors such as small coverage angle and smaller clearance [50]. However, the inclination angle (up to 45º) of the hemispherical cup considered in this study was not large enough to cause edge loading. Moreover, the consideration of edge loading in numerical lubrication analysis involves more complex factors such as starvation. Therefore, the effect of edge loading was not included in this study. This will be considered in future work.

There are other limitations in the present study. Because of the non-symmetric and non-compressible characteristics of the stiffness and flexibility matrices of the complex structure of hip resurfacing system, only 65 × 65 nodes were used for the lubrication analysis due to the extremely high computational cost and storage size requirement for the finer lubrication meshes. As a result, a relatively high viscosity was adopted to facilitate the convergence of numerical solution. It is expected that this issue will be solved using a method of selective-fine-mesh with selective-storage [51]. Moreover, only steady-state condition was considered as the first step to address the importance of the effect of orientation of components. Future work will perform transient analyses.

Conclusions

The EHL of a full MOM hip resurfacing model and three simplified MOM hip resurfacing models were also solved. A flexibility matrix method was used to solve these models. The effects of the orientations of components and the structures of realistic bones on the lubrication performance of MOM hip resurfacing prosthesis were investigated by comparing the full model with the simplified models. It was found that the orientation of the head played a very important role in predicting the pressure distribution and film profile of hip resurfacing prosthesis while the inclination of the cup up to 45° had no appreciable effect on the lubrication performance of MOM hip resurfacing prosthesis. It is expected that the inclination angle of the hemispherical cup may have negligible effect on the wear of hip resurfacing prostheses if the contact area is within the cup (away from the edge). Moreover, the combined effect of material properties and structures of the bones may have a negligible effect.

Acknowledgement

The authors would also like to thank Professor Peiran Yang of Qingdao Technological University for his valuable discussion.

Funding acknowledgement

This work was support by the Overseas Research Students Awards Scheme (ORSAS) to Qingen Meng, the National Natural Science Foundation of China (grant number: 50628505) and the NIHR (National Institute for Health Research) as part of collaboration with the LMBRU (Leeds Musculoskeletal Biomedical Research Unit).

Conflict of interest

The authors have no conflict of interest to disclose for this work.

References

1. Amstutz HC, Grigoris P, Dorey FJ. Evolution and future of surface replacement of the hip. J Orthop Sci 1998; 3: 169-186.

2. Grigoris P, Roberts P, Panousis K, et al. Hip resurfacing arthroplasty: the evolution of contemporary designs. Proc IMechE Part H: J Engineering in Medicine 2006; 220: 95-105.

3. Vassitiou K, Elfick APD, Scholes SC, et al. The effect of 'running-in' on the tribology and surface morphology of metal-on-metal Birmingham hip resurfacing device in simulator studies. Proc IMechE Part H: J Engineering in Medicine 2006; 220: 269-277.

4. Leslie I, Williams S, Brown C, et al. Effect of bearing size on the long-term wear, wear debris, and ion levels of large diameter metal-on-metal hip replacements - An in vitro study. J Biomed Mater Res B 2008; 87B: 163-172.

5. Dowson D, Hardaker C, Flett M, et al. A hip joint simulator study of the performance of metal-on-metal joints - Part 2: Design. Journal of Arthroplasty 2004; 19: 124-130.

6. Langton DJ, Joyce TJ, Jameson SS, et al. Adverse reaction to metal debris following hip resurfacing - The influence of component type, orientation and volumetric wear. Journal of Bone and Joint Surgery-British Volume 2011; 93B: 164-171.

7. Lord JK, Langton DJ, Nargol AVF, et al. Volumetric wear assessment of failed metal-on-metal hip resurfacing prostheses. Wear 2011; 272: 79-87.

8. Mattei L, Puccio FD, Ciulli E. Wear simulation of metal on metal hip replacements: an analytical approach. Proceedings of ASME 2012 11th Biennial Conference on Engineering Systems Design And Analysis: 1-10. Nantes, France. 2012.

9. MHRA. Medical Device Alert MDA/2010/069 (2010).

10. Clarke MT, Lee PTH, Arora A, et al. Levels of metal ions after small- and large-diameter metal-on-metal hip arthroplasty. Journal of Bone and Joint Surgery-British Volume 2003; 85B: 913-917.

11. Daniel J, Ziaee H, Salama A, et al. The effect of the diameter of metal-on-metal bearings on systemic exposure to cobalt and chromium. Journal of Bone and Joint Surgery-British Volume 2006; 88B: 443-448.

12. Moroni A, Savarino L, Cadossi M, et al. Does ion release differ between hip resurfacing and metal-on-metal THA? Clinical Orthopaedics and Related Research 2008; 466: 700-707.

13. Mabilleau G, Kwon YM, Pandit H, et al. Metal-on-metal hip resurfacing arthroplasty: A review of periprosthetic biological reactions. Acta Orthopaedica 2008; 79: 734-747.

14. Shetty VD, Villar RN. Development and problems of metal-on-metal hip arthroplasty. Proceedings of the Institution of Mechanical Engineers Part H-Journal of Engineering in Medicine 2006; 220: 371-377.

15. Glyn-Jones S, Pandit H, Kwon YM, et al. Risk factors for inflammatory pseudotumour formation following hip resurfacing. Journal of Bone and Joint Surgery-British Volume 2009; 91B: 1566-1574.

16. Grammatopoulos G, Pandit H, Kwon YM, et al. Hip resurfacings revised for inflammatory pseudotumour have a poor outcome. Journal of Bone and Joint Surgery-British Volume 2009; 91B: 1019-1024.

17. Kwon YM, Glyn-Jones S, Simpson DJ, et al. Analysis of wear of retrieved metal-on-metal hip resurfacing implants revised due to pseudotumours. Journal of Bone and Joint Surgery-British Volume 2010; 92B: 356-361.

18. Kwon Y-M, Ostlere SJ, McLardy-Smith P, et al. "Asymptomatic" Pseudotumors After Metal-on-Metal Hip Resurfacing Arthroplasty. Journal of Arthroplasty 2011; 26: 511-518.

19. Jin ZM. Theoretical studies of elastohydrodynamic lubrication of artificial hip joints. Proceedings of the Institution of Mechanical Engineers, Part J: Journal of Engineering Tribology 2006; 220: 719-727.

20. Mattei L, Di Puccio F, Piccigallo B, et al. Lubrication and wear modelling of artificial hip joints: A review. Tribology International 2011; 44: 532-549.

21. Udofia IJ, Jin ZM. Elastohydrodynamic lubrication analysis of metal-on-metal hip-resurfacing prostheses. Journal of Biomechanics 2003; 36: 537-544.

22. Liu F, Jin ZM, Roberts P, et al. Importance of head diameter, clearance, and cup wall thickness in elastohydrodynamic lubrication analysis of metal-on-metal hip resurfacing prostheses. Proceedings of the Institution of Mechanical Engineers, Part H: Journal of Engineering in Medicine 2006; 220: 695-704.

23. Meng QE, Liu F, Jin ZM. Elastohydrodynamic lubrication analysis of metal-on-metal hip implants with complex structures using the finite element method. Proceedings of the Institution of Mechanical Engineers, Part J: Journal of Engineering Tribology 2010; 224: 1007-1018.

24. Angadji A, Royle M, Collins SN, et al. Influence of cup orientation on the wear performance of metal-on-metal hip replacements. Proceedings of the Institution of Mechanical Engineers Part H-Journal of Engineering in Medicine 2009; 223: 449-457.

25. De Haan R, Pattyn C, Gill HS, et al. Correlation between inclination of the acetabular component and metal ion levels in metal-on-metal hip resurfacing replacement. Journal of Bone and Joint Surgery-British Volume 2008; 90B: 1291-1297.

26. Hart AJ, Buddhdev P, Winship P, et al. Cup inclination angle of greater than 50 degrees increases whole blood concentrations of cobalt and chromium ions after metal-on-metal hip resurfacing. Hip International 2008; 18: 212-219.

27. Isaac GH, Schmalzried TP, Vail TP. Component mal-position: the 'Achilles' heel' of bearing surfaces in hip replacement. Proceedings of the Institution of Mechanical Engineers Part J-Journal of Engineering Tribology 2009; 223: 275-286.

28. Leslie IJ, Williams S, Isaac G, et al. High Cup Angle and Microseparation Increase the Wear of Hip Surface Replacements. Clinical Orthopaedics and Related Research 2009; 467: 2259-2265.

29. Williams S, Leslie I, Isaac G, et al. Tribology and wear of metal-on-metal hip prostheses: Influence of cup angle and head position. Journal of Bone and Joint Surgery-American Volume 2008; 90A: 111-117.

30. Yew A, Jagatia M, Ensaff H, et al. Analysis of contact mechanics in McKee-Farrar metal-on-metal hip implants. Proceedings of the Institution of Mechanical Engineers Part H-Journal of Engineering in Medicine 2003; 217: 333-340.

31. Udofia I, Liu F, Jin Z, et al. The initial stability and contact mechanics of a press-fit resurfacing arthroplasty of the hip. Journal of Bone and Joint Surgery-British Volume 2007; 89B: 549-556.

32. Dalstra M, Huiskes R, Vanerning L. Development and validation of a 3-dimensional finite-element model of the pelvic bone. Journal of Biomechanical Engineering-Transactions of the ASME 1995; 117: 272-278.

33. Liu F, Udofia IJ, Jin ZM, et al. Comparison of contact mechanics between a total hip replacement and a hip resurfacing with a metal-on-metal articulation. Proceedings of the Institution of Mechanical Engineers Part C-Journal of Mechanical Engineering Science 2005; 219: 727-732.

34. Fan J, Myant C, Underwood R, et al. Synovial fluid lubrication of artificial joints: protein film formation and composition. Faraday Discussions 2012; 156: 69-85.

35. Fan J, Myant CW, Underwood R, et al. Inlet protein aggregation: a new mechanism for lubricating film formation with model synovial fluids. Proceedings of the Institution of Mechanical Engineers Part H-Journal of Engineering in Medicine 2011; 225: 696-709.

36. Myant C, Underwood R, Fan J, et al. Lubrication of metal-on-metal hip joints: The effect of protein content and load on film formation and wear. Journal of the Mechanical Behavior of Biomedical Materials 2012; 6: 30-40.

37. Myant C, Cann PM. In contact observation of model synovial fluid lubricating mechanisms Tribology International 2012: http: // dx.doi.org/10.1016/j.triboint.2012.1004.1029.

38. Cooke AF, Dowson D, Wright V. The rheology of synovial fluid and some potential synthetic lubricants for degenerate synovial joints. Engineering in Medicine 1978; 7: 66-72.

39. Yao JQ, Laurent MP, Johnson TS, et al. The influences of lubricant and material on polymer/CoCr sliding friction. Wear 2003; 255: 780-784.

40. Bergmann G, Deuretzbacher G, Heller M, et al. Hip contact forces and gait patterns from routine activities. Journal of Biomechanics 2001; 34: 859-871.

41. Wang FC, Jin ZM. Elastohydrodynamic lubrication modeling of artificial hip joints under steady-state conditions. Journal of Tribology-Transactions of the ASME 2005; 127: 729-739.

42. Latini F, Forte P. Flexibility matrix method applied to the finite element elastohydrodynamic analysis of plain journal bearings. Proceedings of the Institution of Mechanical Engineers, Part J: Journal of Engineering Tribology 2005; 219: 59-68.

43. Hooke CJ. Special issue on elastohydrodynamic lubrication. Proceedings of the Institution of Mechanical Engineers Part C-Journal of Mechanical Engineering Science 2010; 224: I-II.

44. Piffeteau S, Souchet D, Bonneau D. Influence of thermal and elastic deformations on connecting-rod big end bearing lubrication under dynamic loading. Journal of Tribology-Transactions of the ASME 2000; 122: 181-191.

45. Bonneau D, Guines D, Frene J, et al. EHD analysis, including structural inertia effects and a mass-conserving cavitation model. Journal of Tribology-Transactions of the ASME 1995; 117: 540-547.

46. Liu F, Jin ZM, Grigoris P, et al. Contact mechanics of metal-on-metal hip implants employing a metallic cup with a UHMWPE backing. Proc Inst Mech Eng H 2003; 217: 207-213.

47. Wang FC, Jin ZM. Transient elastohydrodynamic lubrication of hip joint implants. Journal of Tribology-Transactions of the ASME 2008; 130: 011007.

48. Bolland BJRF, Latham JM, Whitwell D. Hip resurfacing Early failures cause concern. British Medical Journal 2012; 341.

49. Fisher J. Bioengineering reasons for the failure of metal-on-metal hip prostheses AN ENGINEER'S PERSPECTIVE. Journal of Bone and Joint Surgery-British Volume 2011; 93B: 1001-1004.

50. Underwood RJ, Zografos A, Sayles RS, et al. Edge loading in metal-on-metal hips: low clearance is a new risk factor. Proceedings of the Institution of Mechanical Engineers Part H-Journal of Engineering in Medicine 2012; 226: 217-226.

51. Xiong SW, Lin C, Wang YS, et al. An Efficient Elastic Displacement Analysis Procedure for Simulating Transient Conformal-Contact Elastohydrodynamic Lubrication Systems. Journal of Tribology-Transactions of the ASME 2010; 132: 021502.

Nomenclature

e_x, e_y, e_z — eccentricity components of femoral head in the *x*, *y* and *z* directions (m)

f_x, f_y, f_z — calculated load components in the *x*, *y* and *z* directions, respectively (N)

h — film thickness (m)

p — hydrodynamic pressure (Pa)

R_c — radius of acetabular cup (m)

R_h — radius of femoral head (m)

w_x, w_y, w_z — applied load in the *x*, *y* and *z* directions, respectively (N)

x, y, z — Cartesian coordinates

β — inclination angle of cup (degree)

δ — local elastic deformation of bearing surfaces (m)

η — viscosity of synovial fluid (Pa·s)

ϕ, θ — spherical coordinates (degree)

ω_x, ω_y, ω_z — angular velocities around the *x*, *y* and *z* axes, respectively (rad/s)

Captions

Figure 1 (a) Schematic diagram of a full MOM hip resurfacing arthroplasty model; (b) the cross section of the full model shown in Figure 1(a)

Figure 2 Schematic diagram of the inclined ball-in-socket model for the lubrication analysis of hip resurfacing system

Figure 3 Definition of spherical coordinates and lubrication grid under spherical coordinates

Figure 4 Finite-element models to calculate the stiffness matrices of the lubrication nodes of the full hip resurfacing replacement: the pelvis and cup (a); the proximal femur and head (b)

Figure 5 Schematic diagrams of simplified models: (a) detailed structure of simplified models; (b) cross section of model-s1, a horizontally positioned cup and a vertically positioned head; (c) cross section of model-s2, both the cup and the head were inclined to simulate an anatomical contact; (d) cross section of model-s3, the cup was inclined but the head was vertical

Figure 6 Contour plots of the hydrodynamic pressure (MPa) of model-f (a), model-s1 (b), model-s2 (c) and model-s3 (d)

Figure 7 Contour plots of the film thickness (μm) of model-f (a), model-s1 (b), model-s2 (c) and model-s3 (d)

Figure 8 The pressure distribution and film thickness on the lines of $\phi = 90^{\circ}$ (a, b) and $\theta = 90^{\circ}$ (c, d) of the full hip resurfacing EHL model and simplified models

Figure 9 Dry contact pressure distribution (MPa) of simplified models: model-s1 (a), model-s2 (b) and model-s3 (c) respectively, under a vertical load of 3200 N

Figure 10 The pressure distribution and film thickness on the lines of ϕ = 90º (a, b) and θ = 90º (c, d) of the full hip resurfacing EHL model and reference models

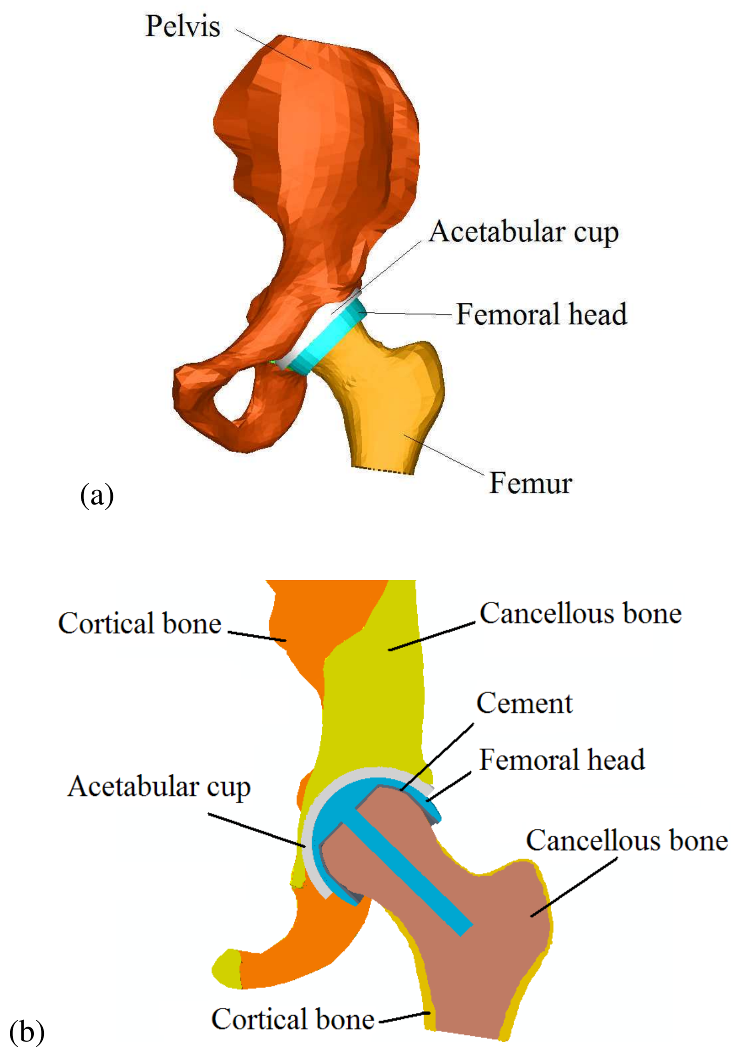

Figure 1 (a) Schematic diagram of a full MOM hip resurfacing arthroplasty model; (b) the cross section of the full model shown in Figure 1(a)

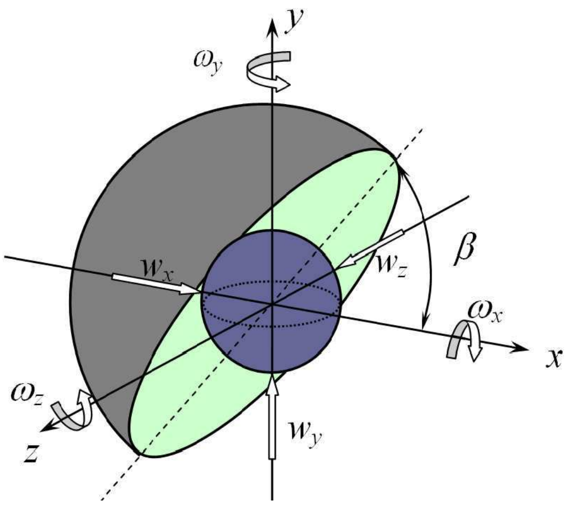

Figure 2 Schematic diagram of an inclined ball-in-socket model for the lubrication analysis of hip resurfacing system

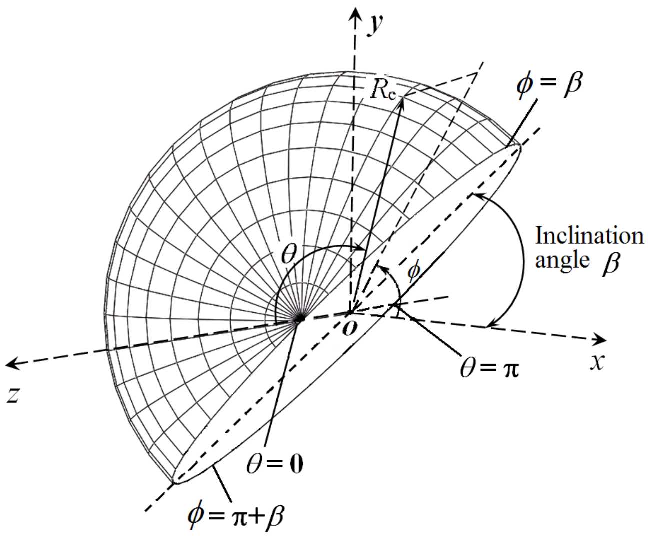

Figure 3 Definition of spherical coordinates and lubrication grid under spherical coordinates

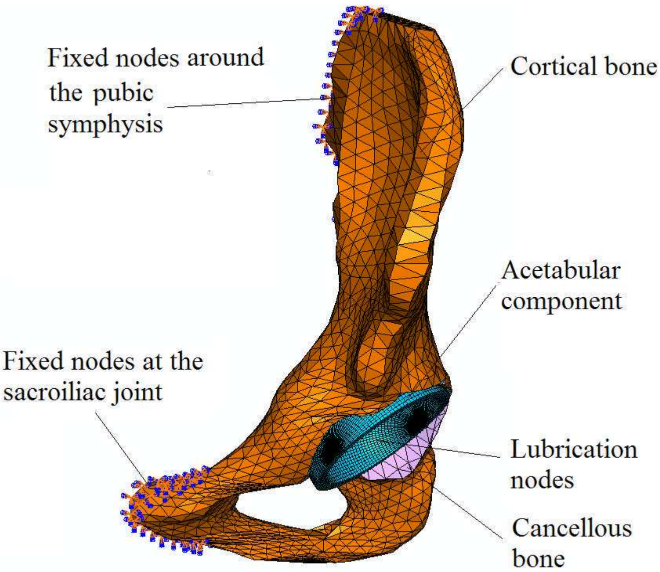

(a)

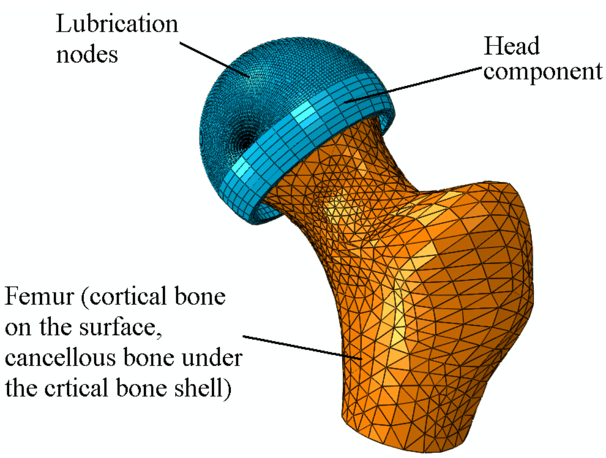

(b)

Figure 4 Finite-element models to calculate the stiffness matrices of the lubrication nodes of the full hip resurfacing replacement: the pelvis and cup (a); the proximal femur and head (b)

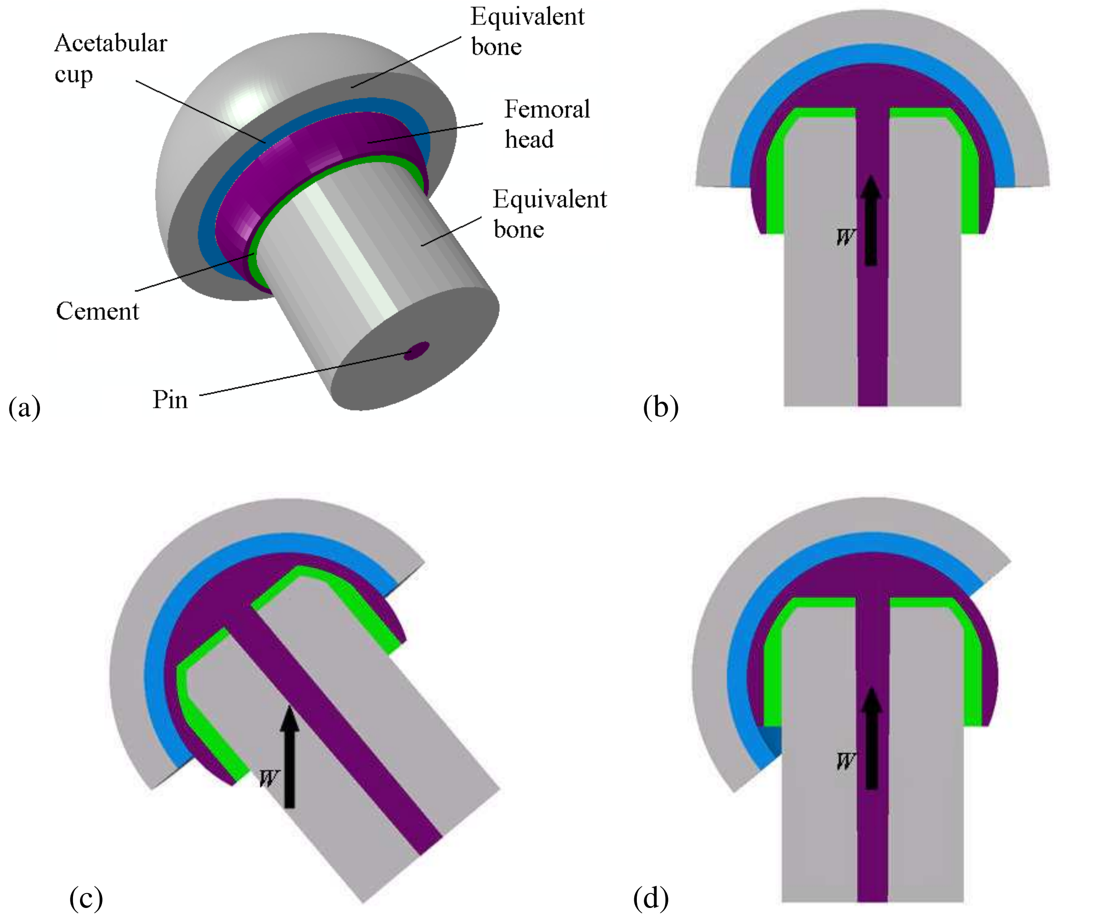

Figure 5 Schematic diagrams of simplified models: (a) detailed structure of simplified models; (b) cross section of model-s1, a horizontally positioned cup and a vertically positioned head; (c) cross section of model-s2, both the cup and the head were inclined to simulate an anatomical contact; (d) cross section of model-s3, the cup was inclined but the head was vertical

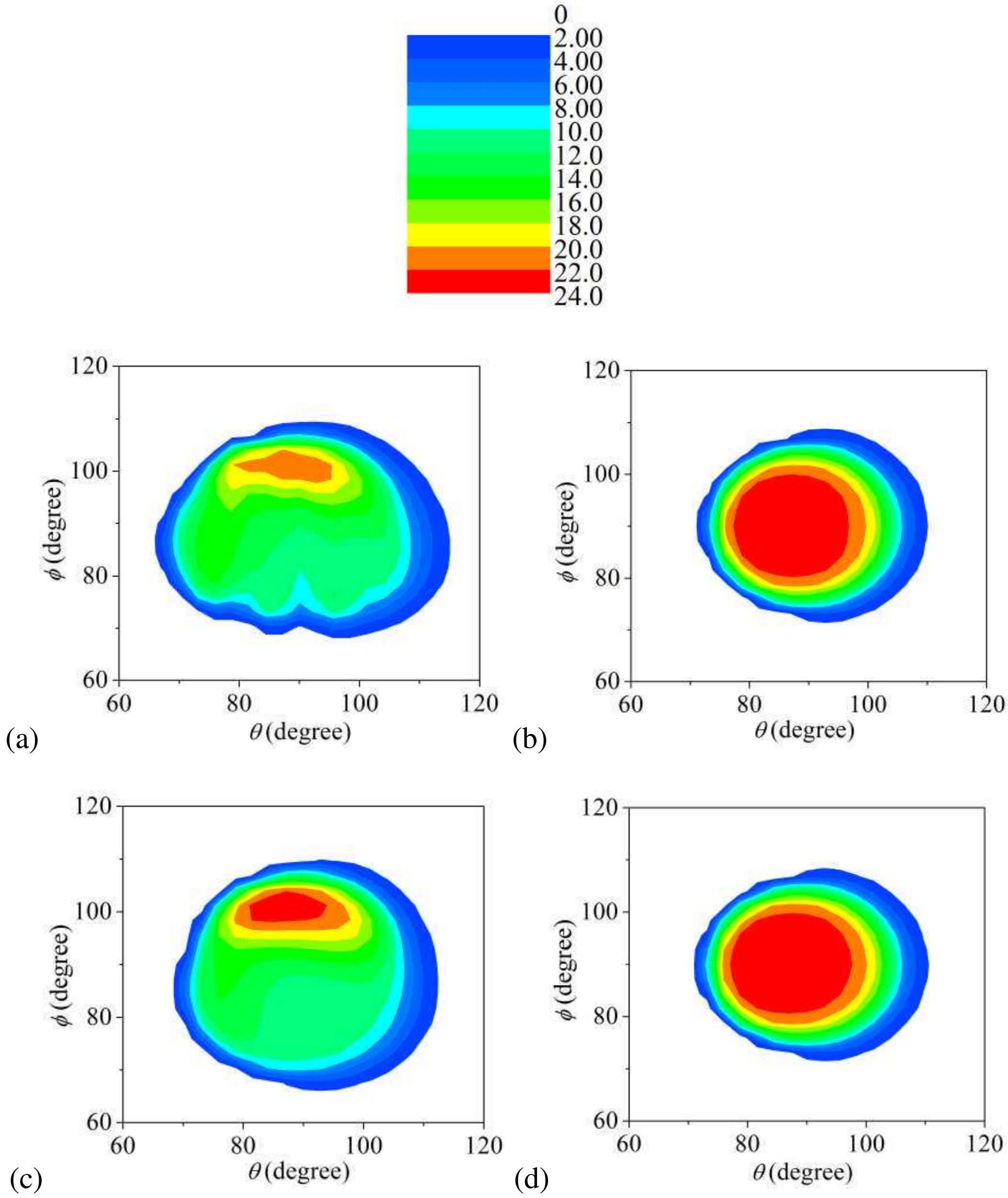

Figure 6 Contour plots of the hydrodynamic pressure (MPa) of the full hip resurfacing model (a), model-s1 (b), model-s2 (c) and model-s3 (d)

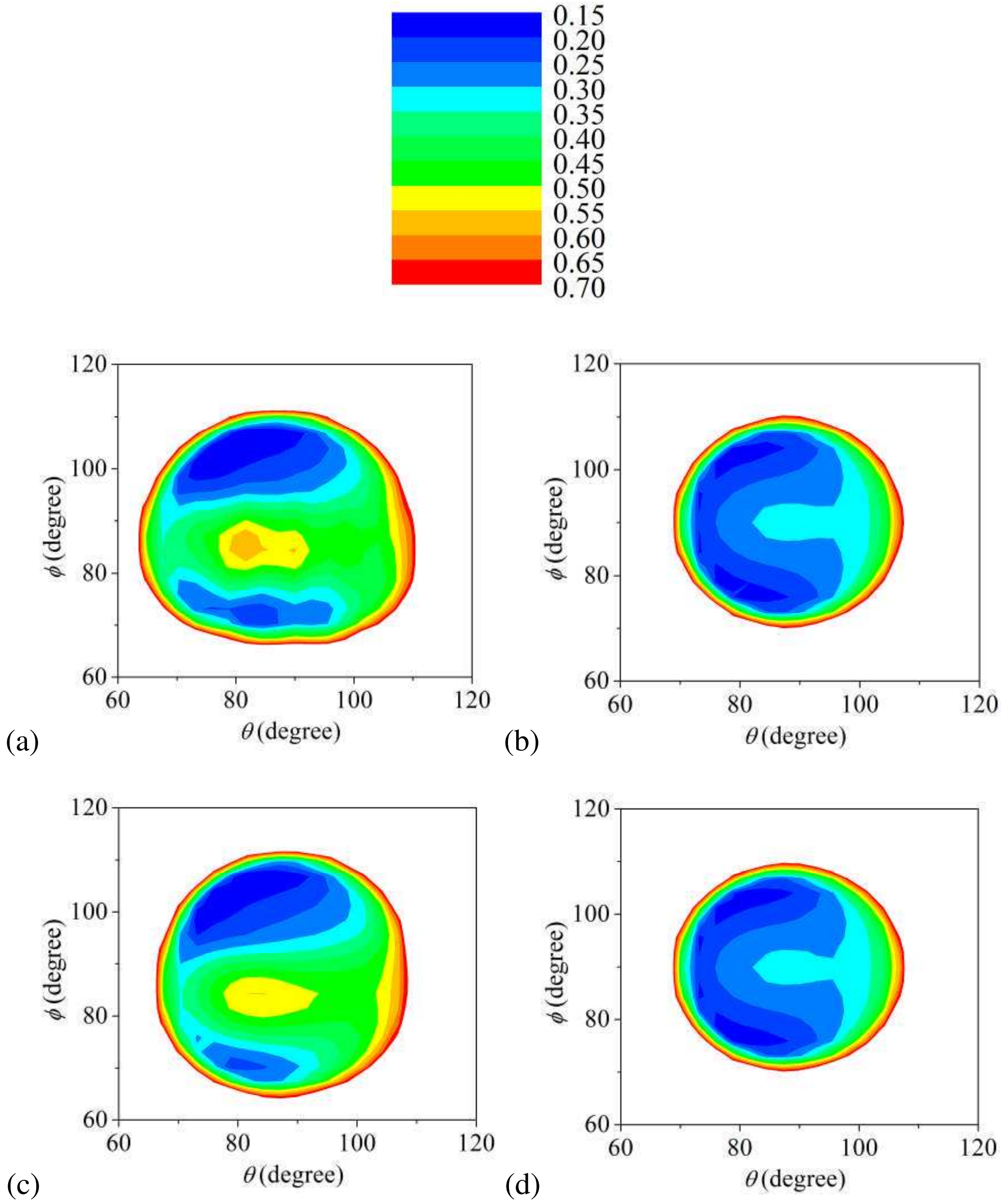

Figure 7 Contour plots of the film thickness (µm) of the full hip resurfacing model (a), model-s1 (b), model-s2 (c) and model-s3 (d)

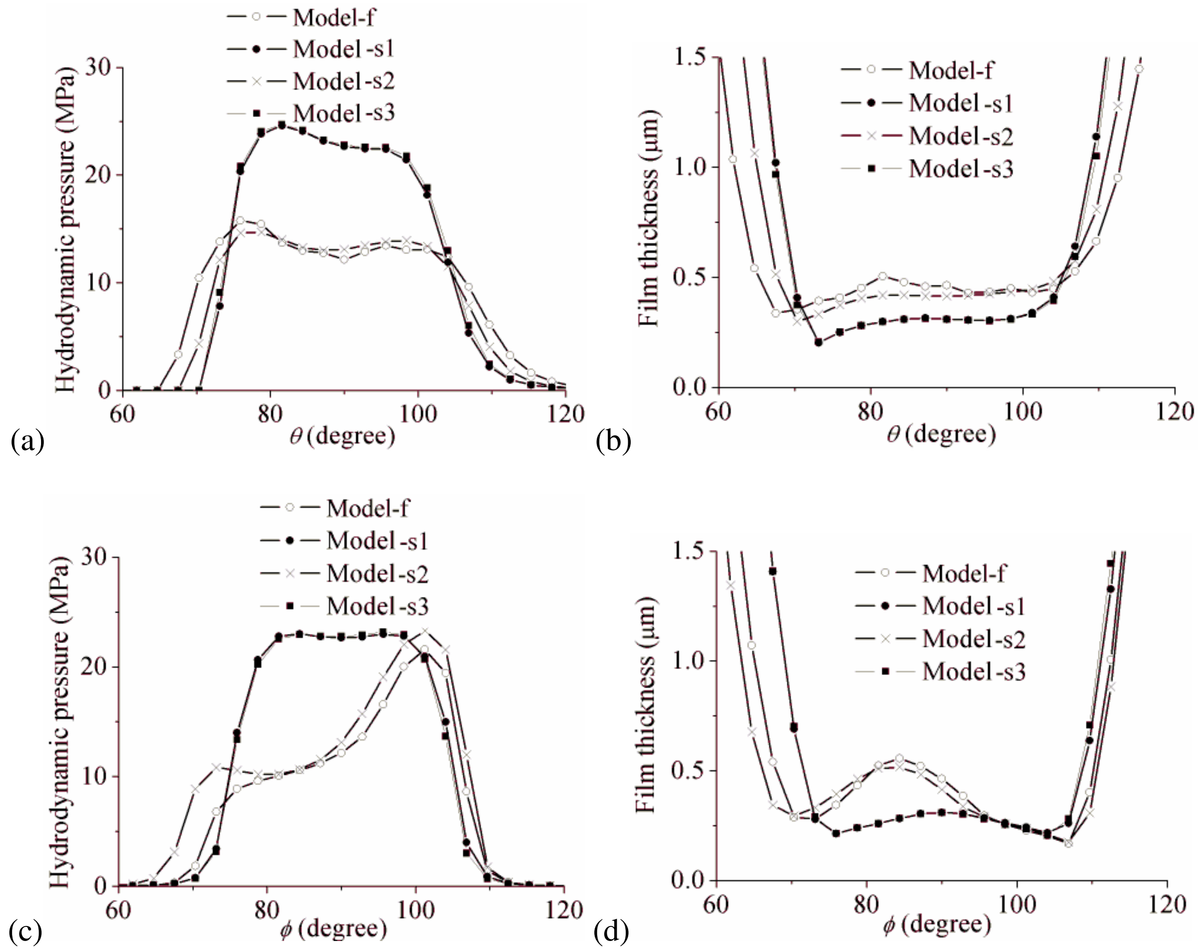

Figure 8 The pressure distribution and film thickness on the lines of $\phi = 90º$ (a, b) and $\theta = 90º$ (c, d) of the full hip resurfacing EHL model and simplified models

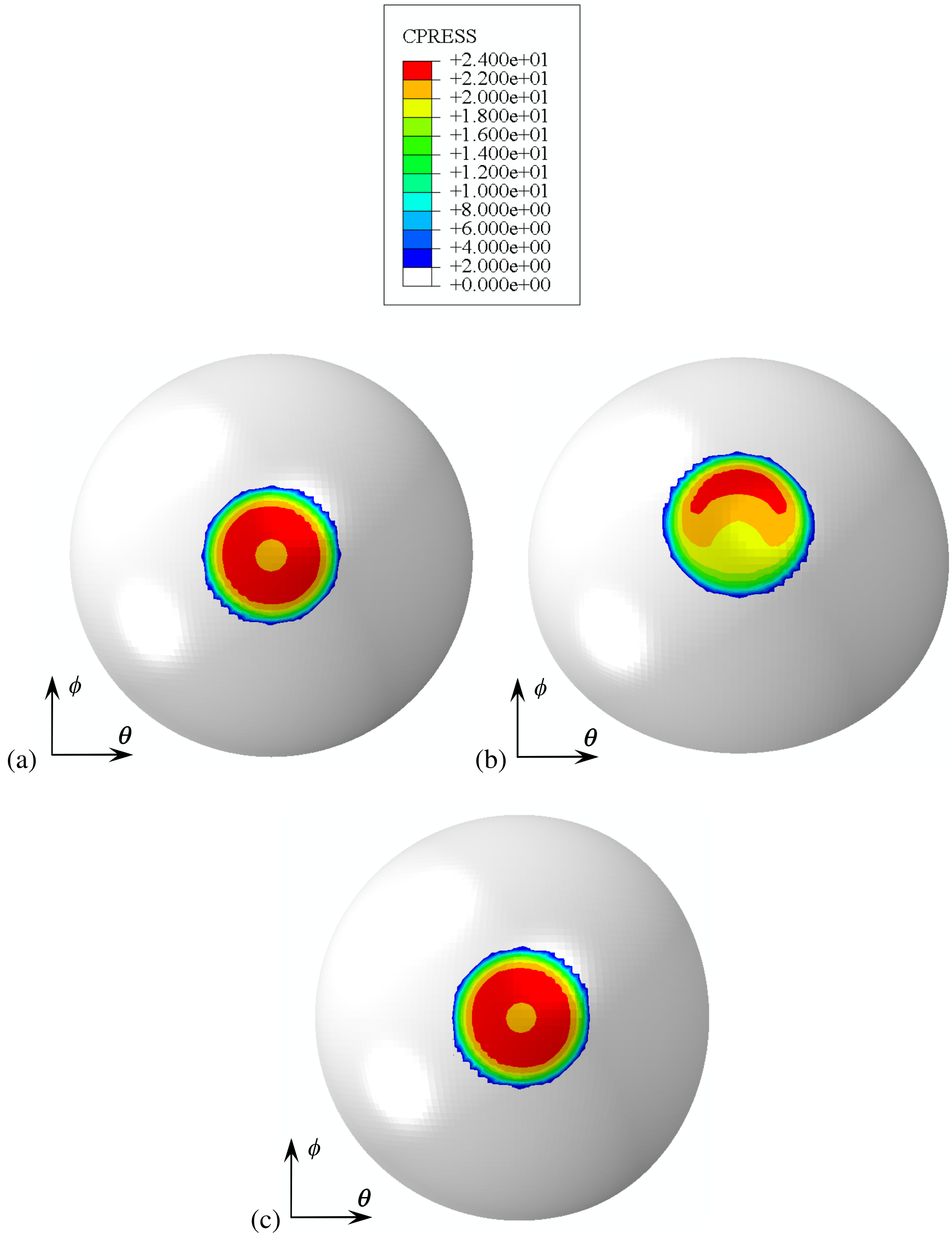

Figure 9 Dry contact pressure distribution (MPa) of simplified models: model-s1 (a), model-s2 (b) and model-s3 (c), respectively, under a vertical load of 3200 N

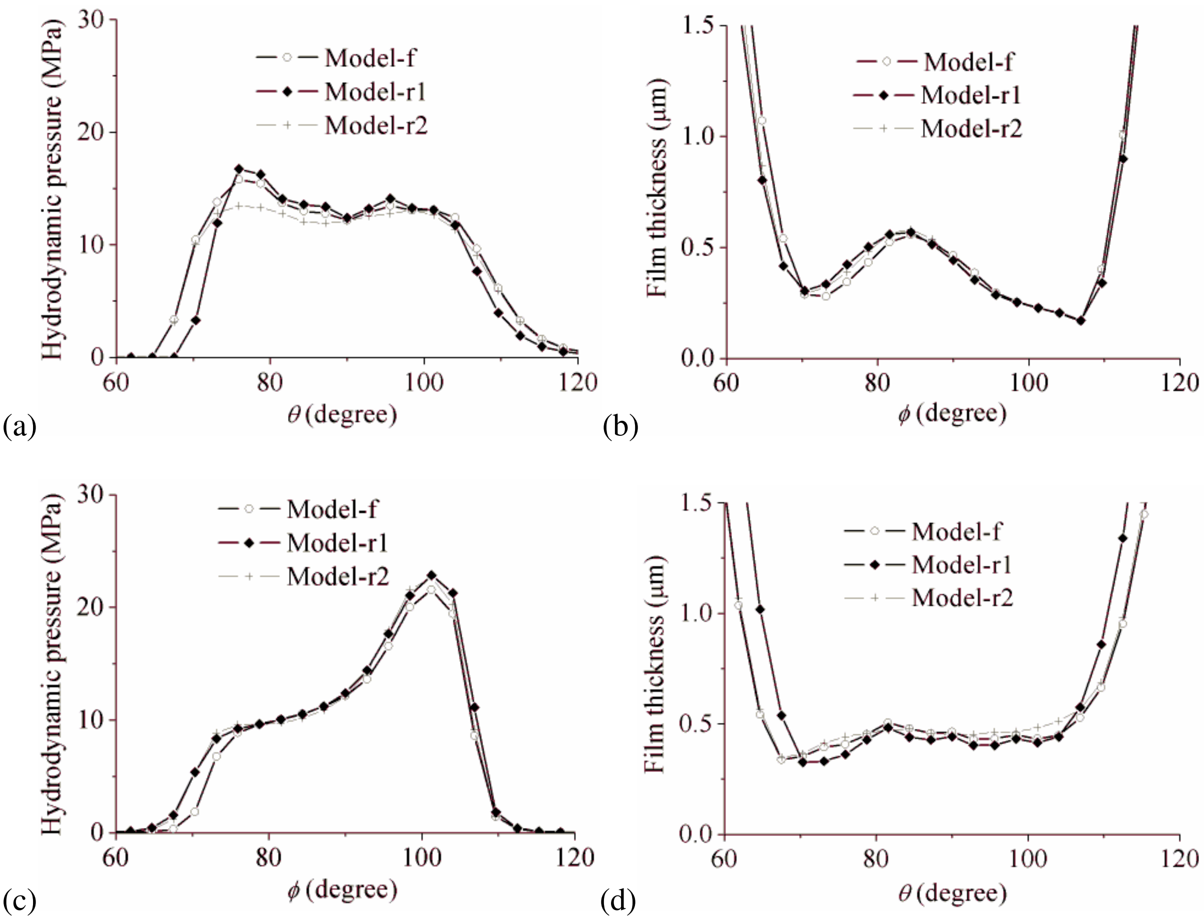

Figure 10 The pressure distribution and film thickness on the lines of $\phi = 90°$ (a, b) and $\theta = 90°$ (c, d) of the full hip resurfacing EHL model and reference models